A Tactile-based Framework for Active Object Learning and Discrimination using Multi-modal Robotic Skin

Mohsen Kaboli [1], Di Feng[1], Kunpeng Yao[1], Pablo Lanillos[1], Gordon Cheng[1]

***Abstract*—In this paper, we propose a complete probabilistic tactile-based framework to enable robots to autonomously explore unknown workspaces and recognize objects based on their physical properties. Our framework consists of three components: (1) an active pre-touch strategy to efficiently explore unknown workspaces; (2) an active touch learning method to learn about unknown objects based on their physical properties (surface texture, stiffness, and thermal conductivity) with the least number of training samples; and (3) an active touch algorithm for object discrimination, which selects the most informative exploratory action to apply to the object, so that the robot can efficiently distinguish between objects with a few number of actions. Our proposed framework was experimentally evaluated using a robotic arm equipped with multimodal artificial skin. The robot with the active pre-touch method reduced the uncertainty of the workspace up to 30% and 70% compared to uniform and random strategies, respectively. By means of the active touch learning algorithm, the robot used 50% fewer samples to achieve the same learning accuracy than the baseline methods. By taking advantage of the prior knowledge obtained during the learning process, the robot actively discriminated objects with an improvement of 10% recognition accuracy compare to the random action selection approach.**

***Index Terms*—Active tactile learning, tactile object recognition, force and tactile sensing, artificial robotic skin.**

I. Introduction and Related Work

HUMANS use the sense of touch to actively explore environment and objects through their various physical properties such as surface texture, stiffness, shape, and thermal conductivity. To this end, we strategically select the tactile exploratory actions to efficiently learn about objects and discriminate among them [1]. For instance, sliding to sense the textural properties, pressing to estimate the stiffness, and static contact to measure the thermal conductivity.

Tactile sensing in robotics has been investigated for several decades and current tactile sensors can provide rich and direct tactile feedback to the robotic systems [2]. A robot with the sense of touch can explore the environment and perceive valuable information which cannot be acquired through, for instance, visual feedback [3]–[6]. Previous researchers have used various robotic system with different tactile sensors to passively explore objects and discriminate among them through their physical properties [7]–[14]. In these works, the exploratory movements have been predefined. Therefore, the autonomy of the robot is limited. In this sense, active tactile exploration has shown great potential for enabling the robotic system with more natural and human-like strategies for the task of object discrimination. In order to actively discriminate among objects, Xu *et al.* used the index finger of the Shadow Hand with the BioTac sensor to collect training data by executing three different exploratory actions five times on each experimental object [15]. They constructed and employed observation models to discriminate among objects through a sequence of different exploratory movements. However, the base and wrist of the dexterous robotic hand were fixed on a table, and all joints in the hand and wrist were deactivated (except two joints of the index finger). Therefore, these physical constraints result in a method which is highly likely unscalable for robotic tactile exploration.

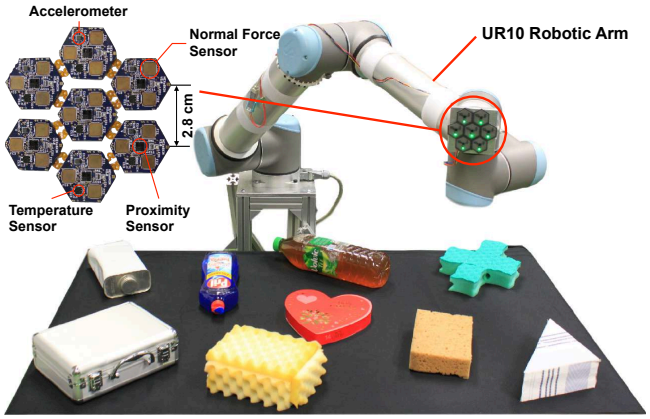

Fig. 1. Experimental setup. The UR10 robotic arm mounted with the multi-modal artificial skin on its end-effector.

In [16], a biomimetic fingertip was controlled to slide on 10 different surfaces to perceive their textural properties. In order to actively discriminate among the surfaces, the observation models were built offline with uniformly sampled training data of each surface texture under a range of contact depths. In all the above mentioned work and other similar studies in [17]–[20], the location and orientation of the experimental objects in the workspace were known. Moreover, the training samples were collected offline in order to construct the observation models for each object. To increase the autonomy of a robotic system during the tactile-based object recognition, the robot

[1]Authors are with the Institute for Cognitive Systems (ICS), Technische Universität München, Germany Email: mohsen.kaboli@tum.de

Manuscript received: February 15, 2017; Revised May 11, 2017; Accepted June 13, 2017.

This paper was recommended for publication by Editor John Wen upon evaluation of the Associate Editor and Reviewers' comments.

The video to this paper can be found via the link: http://web.ics.ei.tum.de/~mohsen/videos/RAL2017.mp4

Digital Object Identifier (DOI): see top of this page

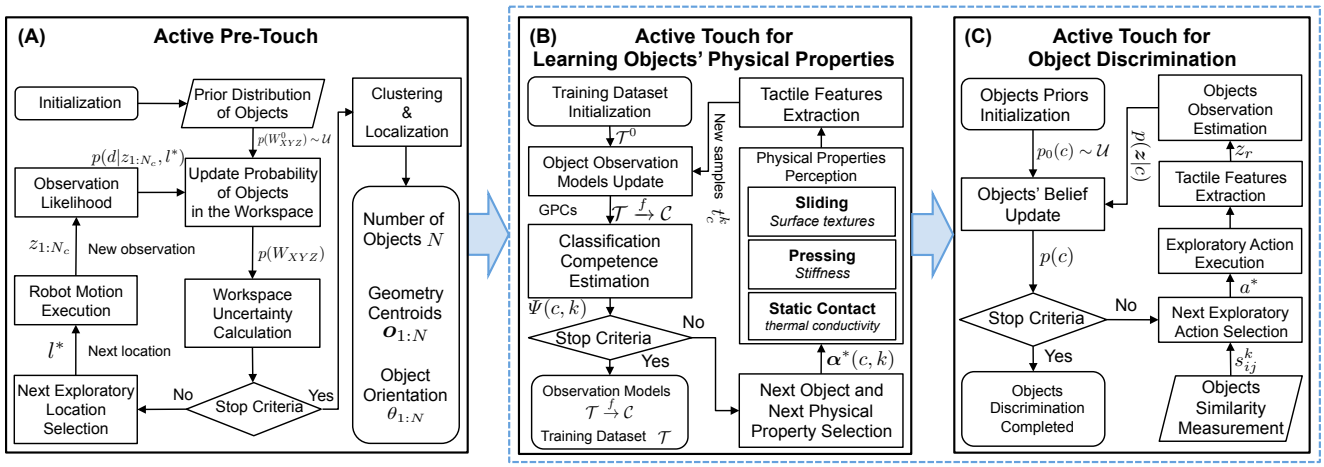

Fig. 2. Proposed Tactile-based Framework.

should be able to autonomously explore unknown workspace, actively detect the number of objects as well as estimate their positions in the workspace. Moreover, the informativeness of training data obtained with each object is different. Some objects have discriminant tactile properties that make them easily to be identified from the others. Therefore, collecting too many training samples with these objects is redundant, whereas for objects, which are easily confused with each other due to their similar properties, it is necessary to collect sufficient samples to construct reliable and robust observation models. Furthermore, to efficiently discriminate among objects the autonomous robot should strategically select and execute the exploratory actions that provide the robotic system with the maximum informativeness.

A. *Contribution*

To tackle the aforementioned problems, we propose a probabilistic pre-touch and touch based framework (see Fig. 2) to enable robotic systems to autonomously explore unknown workspace, actively learn about objects' properties, and to efficiently discriminate among objects by means of their physical properties. Our contribution is three fold: 1) An active pre-touch approach to enable the robotic systems to autonomously and efficiently explore the unknown workspace in order to calculate the number of objects, find their location, and estimate their orientation (see Fig. 2-A); 2) An active touch method to learn the physical properties of objects (surface textures, stiffness, and thermal conductivity) with the least possible number of training samples in order to construct reliable objects' observation models (see Fig. 2-B); 3) An active touch method to efficiently discriminate among objects with a smaller number of exploratory actions (sliding, pressing, and static contact) (see Fig. 2-C).

II. System Description

A. *Multi-modal Artificial Skin*

In order to emulate a human sense of touch, we have designed and manufactured multi-modal artificial skin [21] to provide robotic systems with the ability of pre-touch and sense of touch. Each skin cell has one micro controller and a set of multi-modal tactile sensors, including one *proximity sensor* (pre-touch), one *three-axis accelerometer*, one *temperature sensor*, and three *normal-force sensors* (see Table I). All the skin cells are directly connected with each other via bendable and stretchable inter-connectors.

TABLE I
THE MULTI-MODAL ROBOTIC SKIN CHARACTERISTICS.

Modality	Acceleration	Force	Proximity	Temperature
Per Cell	1	3	1	1
Range	$\pm 2\,g$	$> 0 - 10\,N$	$1 - 200\,mm$	$-40 - 150\,^{\circ}\mathrm{C}$
Bandwidth	$0 - 1\,kHz$	$0 - 33\,kHz$	$0 - 250\,Hz$	$0 - 7\,Hz$

B. *Robotic System*

We mounted one skin patch on the end-effector of the 6-DoF industrial robot called UR10 (Universal Robots). The skin patch consists of 7 skin cells including: 7 proximity sensors, 7 three-axis accelerometer sensors, 7 temperature sensors, and 21 normal-force sensors (see Fig. 1).

III. Active Pre-Touch for Workspace Exploration

We propose an active pre-touch probabilistic approach for robotic systems with the proximity sensors to efficiently explore an unknown workspace. This method reduces the number of exploratory movements and measurements required to localize objects in the workspace. Then, the robot is able to estimate the number of objects, their poses, and their geometric centroids.

A. *Problem Definition*

The workspace W_{XYZ} is defined as a discretized 3D grid bounded by the reaching capabilities of the robot (see Fig. 3). The artificial skin of the robot has an array of N_c proximity sensors with known locations $l^n_{1:N_c}$ with respect to the end-effector position l^n at each observation n. The sensor array outputs a set of measurements $z^n_{1:N_c}$. To take into account the non-linearities and the uncertainty associated with those

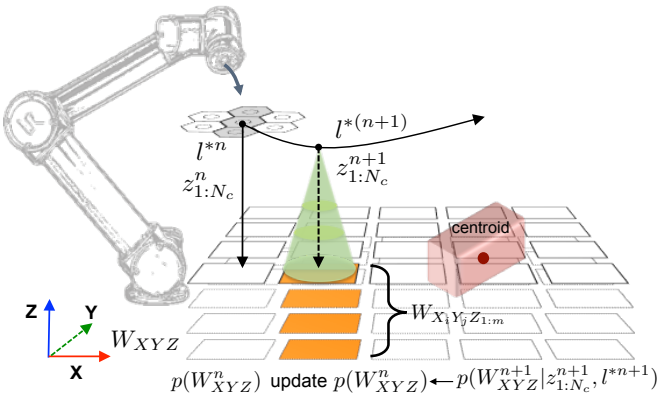

Fig. 3. An illustration of active pre-touch process.

measurements, we compute the distance d^n between the skin cells and the object as the probability $p(d^n|z_i^{1:n}, l^{1:n})$ (for ith proximity sensor given all previous measurements).

Finally, we define $p(W^n_{XYZ})$ as the probability of the presence of an object in every cell of the workspace at the nth observation. The initial $p(W^0_{XYZ})$ is a uniform distribution that will be updated using the new measurements. We assume that the robot's end-effector is horizontal to the X-Y plane of the workspace.

B. Methodology

First, the robot starts the exploration from a fixed location corresponding to a grid edge. Then, it generates a set of potential next end-effector locations $l^{n+1} \in L^{n+1}$, i.e., the centre of each neighbouring grid cell. Afterwards, it selects the one that maximizes the probability of detecting an object. The robot performs the next movement and uses the new sensor measurements $z^n_{1:N_c}$ to update $p(W^n_{XYZ})$. This process will be iteratively executed until the robot is certain about the workspace, e.g., the entropy of $p(W^n_{XYZ})$ is below 1%. In order to fuse the measurements taken from all sensors of the array we assume that their readings are independent of each other. The joint probability distribution is given by:

$$p(d^n|z^{1:n}_{1:N_c}, l^{1:n}) \propto \prod_{i=1}^{N_c} p(z_i^n|l^n, d^n) p(d^{n-1}|z^{1:n-1}, l^{1:n-1}) \quad (1)$$

Where $p(z_i^n|l^n, d^n)$ is the likelihood of having measurement z^n given that the object is at distance d^n and the end-effector is at l^n. This is obtained experimentally (see VII-B1). As the end-effector is moving on X-Y plane, d^n corresponds to the cells of $W_{X_iY_jZ_{1:m}}$, where i and j are defined by the end-effector's location l^n and $Z_{1:m}$ are the cells below l^n (m is the number of cells in Z direction, the orange colored cells in Fig. 3).

*1) **Next Exploratory Location**:* In order to compute the next best location l^{*n+1} of the end-effector, we employ a method based on [22], [23] proposed for air vehicles with radar, which in this study we modified it to be used with an array of proximity sensors. Considering that the end-effector is moving on X-Y plane, we define the current estimate of the 2D workspace as $p(W^n_{XY})$. The best next end-effector location l^{*n+1} is the one that maximizes the probability of detecting an object in the workspace:

$$l^{*n+1} = \arg \max_{l^{n+1} \in L^{n+1}} \sum_{W_{XY}} p(z^{n+1}_{1:N_c} = D|l^{n+1}, W^{n+1}_{XY}) p(W^n_{XY}) \quad (2)$$

where $p(z^{n+1}_{1:N_c} = D|l^{n+1}, W^{n+1}_{XY})$ is the probability of detecting an object given the next location l^{n+1}, which for every proximity sensor i (for the skin patch i =1,...,7) is modelled using the following exponential function:

$$p(z_i^{n+1} = D|l^{n+1}, W^{n+1}_{XY}) = P_{max}\ e^{-\sigma\left(\frac{\|l^n - W^n_{X_iY_j}\|}{d_{max}}\right)^2} \quad (3)$$

where $\|\cdot\|$ is the Euclidean distance and $W_{X_iY_j}$ defines the center position of each grid cell in X-Y plane. $P_{max} \in (0,1)$ (in this study P_{max} = 0.9) is the maximum probability of detecting an object with the proximity sensor, and d_{max} (d_{max} = 5 cm) and σ (σ = 0.6) shape the maximum coverage of the sensor cone in the workspace grid (green cone in Fig. 3). In order to update $p(W^n_{XY})$, via recursive Bayesian estimation, we assume that the observations $z^n_{1:N_c}$ are non-object detection (Fig. 3).

*2) **Objects clustering and centroid estimation**:* First, the final $p(W^n_{XYZ})$ is thresholded (e.g. 0.9 probabilty) obtaining a binary 3D matrix where 0 is a no-object and 1 is an object. Then, we estimate the number of objects k using a three dimensional connected-labeling algorithm and removing the small clusters (one grid cell) that are unconnected regions of objects. The cells are considered connected if they are adjacent following the 26-connected neighborhood pattern. In order to include all the occupied regions and not only the connected ones, the number of objects found is used to initialize the k-means algorithm that computes the 3D bounding box of each object. Finally, the pose and the geometric centroid of each object are extracted by means of its bounding box.

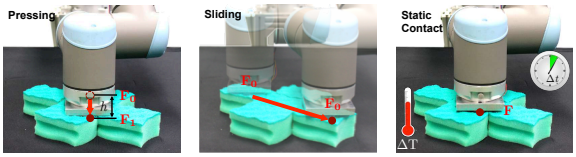

Fig. 4. Exploratory actions: pressing, sliding, and static contact

IV. Object Physical Properties Perception

A robotic system with the sense of touch needs to execute various exploratory actions on the objects to perceive their physical properties as a human does. For instance, a robot slides its sensitive area on the object's surface to sense its textural property, presses on an object to measure its stiffness, and performs static contact with an object to estimate its thermal conductivity.

***Stiffness**:* The robot measures the stiffness of an object by pressing on the object (see Fig. 4). To do this, UR10 with artificial skin on its end-effector first establishes a light contact with the objects. The light contact is detected as soon as the measured normal force averaged over all sensors F_{av}=$\frac{1}{N_c N_r}\sum_{n_c=1}^{N_c}\sum_{n_r=1}^{N_r} F_{n_c,n_r}$ exceeds a threshold f_ε, i.e. $F_{av} > f_\varepsilon$ ($N_c = 7$ is the number of skin cell and N_r=3 is the number

of normal force sensors in each skin cell). Afterwards, the UR10 with its sensitive end-effector presses the top surface of the object. For all normal force sensors F_{n_c,n_r}, the difference between the forces recorded before and after pressing ($\Delta F_{n_c,n_r}$) is used as an indication of the stiffness on the local contact area. The averaged difference value over all force sensors serves as a measurement of stiffness of the object $\frac{1}{N_c N_r}\sum_{n_c=1}^{N_c}\sum_{n_r=1}^{N_r}\Delta F_{n_c,n_r}$.

***Textural Properties**:* To perceive textural properties of objects, the robotic system equipped with the artificial skin slides its sensitive part on the surface of objects. In this study, the vibrations generated during the sliding movement are measured by the three-axis accelerometer in each skin cell. To extract tactile feature from the output of each axis of accelerometer sensors ($a^x_{n_c}$, $a^y_{n_c}$, $a^z_{n_c}$), we proposed in [24], [25] a set of tactile feature descriptors. Our proposed tactile descriptors represent the statistical properties of the tactile signals in the time domains (see Table II). $A(s_n)$ is the total power of a signal. $M(s_n)$ is the square root of the ratio of the variance of the first derivative of the signal to that of the signal. $C(s_n)$ is the second derivative of the variance and shows how the shape of the signal is similar to a pure sine wave. $L(s_n, v_n)$ is the linear correlations between each axis of the accelerometer. In this study, the proposed tactile descriptors for N_c number of skin cells are defined as $\mathbf{A}_{total}$, $\mathbf{M}_{total}$, and $\mathbf{C}_{total}$, and $\mathbf{L}_{total}$ in Table II. In all equations, s_n and v_n are the output of each axis of the accelerator. The final proposed tactile descriptor (TD) is the concatenation of the all descriptors, which can be written as: $\mathbf{TD} = [\mathbf{A}_{total};\ \mathbf{M}_{total};\ \mathbf{C}_{total};\ L_{total}]$.

TABLE II
TACTILE FEATURE DESCRIPTORS

$A(s_n) = \frac{1}{N}\sum_{n=1}^{N}(s_n - \bar{s})^2$
$M(s_n) = \left(A(\frac{ds_n}{dn})/A(s_n)\right)^{-1/2}$
$C(s_n) = M(\frac{ds_n}{dn})/M(s_n)$
$L(s_n, v_n) = \sum_{n=1}^{N}(s_n - \bar{s})(v_n - \bar{v})/\sigma(s_n)\sigma(v_n)$
$\mathbf{A}_{total} = \left[\sum_{n_c=1}^{N_c}\frac{A(a^x_{n_c})}{N_c}, \sum_{n_c=1}^{N_c}\frac{A(a^y_{n_c})}{N_c}, \sum_{n_c=1}^{N_c}\frac{A(a^z_{n_c})}{N_c}\right]$
$\mathbf{M}_{total} = \left[\sum_{n_c=1}^{N_c}\frac{M(a^x_{n_c})}{N_c}, \sum_{n_c=1}^{N_c}\frac{M(a^y_{n_c})}{N_c}, \sum_{n_c=1}^{N_c}\frac{M(a^z_{n_c})}{N_c}\right]$
$\mathbf{C}_{total} = \left[\sum_{n_c=1}^{N_c}\frac{C(a^x_{n_c})}{N_c}, \sum_{n_c=1}^{N_c}\frac{C(a^y_{n_c})}{N_c}, \sum_{n_c=1}^{N_c}\frac{C(a^z_{n_c})}{N_c}\right]$
$\mathbf{L}_{total} = \left[\sum_{n_c=1}^{N_c}\frac{L(a^x_{n_c},a^y_{n_c})}{N_c}, \sum_{n_c=1}^{N_c}\frac{L(a^x_{n_c},a^z_{n_c})}{N_c}, \sum_{n_c=1}^{N_c}\frac{L(a^y_{n_c},a^z_{n_c})}{N_c}\right]$

***Thermal Conductivity**:* A robotic system with tactile sensing can identify objects through thermal cues by applying static contact on them. When measuring the object's thermal conductivity, the robot contacts its sensitive part with the object surface for a certain time period $t_{contact}$, during which the average temperature time series of the contacted area is recorded by temperature sensors: T_{total}=$\{\frac{1}{N_c N_T}\sum_{n_c=1}^{N_c}\sum_{n_T=1}^{N_T}T^i_{n_c,n_T}\}_{i=1}^{t_{contact}}$, where N_T is the number of temperature sensors in each skin cell, and T_{n_c,n_T} represents the recordings of a temperature sensor. The final thermal feature (TF) is the combination of the average temperature time series and its gradient at each time step $TF = [T_{total}, \Delta T_{total}]$.

V. ACTIVE TOUCH FOR LEARNING PHYSICAL PROPERTIES (AT-LPP)

In this section, we describe our proposed probabilistic method for active tactile object learning. Our proposed algorithm enables a robotic system to efficiently learn about objects via their physical properties and to correspondingly construct the observation models of the objects. We start with formalizing the active tactile learning problem. Then, we describe in detail our proposed algorithm called Active Touch for Learning Physical Properties (AT-LPP).

A. Problem Definition

Suppose that there are N objects ($\mathscr{C} = \{c_i\}_{i=1}^{N}$) in the workspace with the known poses. We denote the physical properties of objects by $\mathscr{K} = \{k_j\}_{j=1}^{K}$. These objects may have similar physical properties, for instance similar surface textures, while some might have quite different properties, for example different stiffness and thermal conductivity. In this scenario, the task of the robot is to efficiently learn about objects by means of their physical properties with as few training samples as possible and to efficiently construct the reliable observation models of the objects. Since the objects with the similar properties cannot be easily distinguished from each other, the robot should autonomously collect more training samples with these objects. The active tactile learning problem is formulated as a standard supervised learning problem for multi-class classification, where each object is regarded as a class; for each tactile property, a probabilistic classifier is efficiently constructed by iteratively selecting the *next object to explore* and the *next physical property to learn*, in order to collect the next training sample. In our proposed active learning algorithm the one versus all (OVA) Gaussian Process Classifier (GPC) is employed to construct observation models of objects. GPC trains the function $\mathscr{X} \xrightarrow{f} \mathscr{Y}$, where $\mathscr{X}$ is the observation set and $\mathscr{Y}$ is the target set which contains integers indicating the labels of the input data, $\mathscr{Y} = \{1, 2, 3, ..., N\}$. Given a new sample $\boldsymbol{x}^*$, the observation probability of a class $p(y|\boldsymbol{x}^*)$ can be estimated by $f(\boldsymbol{x}^*)$. In this paper we used RBF [26] as the covariance function and its hyper-parameters are selected through cross-validation.

B. Methodology

The robot starts the learning process by building a training dataset with a small number of samples ($\mathscr{T} = \{\mathscr{T}_{k_j}\}_{j=1}^{K}$, where k_j represents a physical property of objects). Then the robot iteratively collects new training data. At each iteration, AT-LPP algorithm updates GPCs with the training data set collected thus far, and estimates the uncertainty in the constructed observation models (classification competence estimation) which guide to next round of tactile data collection. Using AT-LPP the robot enlarges the training dataset by greedily sampling the next object and the next property which may bring the largest improvement to the performance of GPCs. The learning process is repeated until a target criteria is reached, in our case, when there is no improvement of the uncertainty of GPCs. Finally, the robotic system constructs reliable observation models of the objects by using the efficiently collected

training dataset. Fig. 2 shows the entire process of the AT-LPP algorithm.

*1) **Classification Competence Estimation**:* In order to estimate the GPCs competence, AT-LPP measures the Shannon entropy of each training sample $\boldsymbol{t} \in \mathscr{T}$: $\mathscr{H}(c|\boldsymbol{t}) = -\sum_{c\in\mathscr{C}} p(c|\boldsymbol{t})\log(p(c|\boldsymbol{t}))$. Then the training dataset of one property $\mathscr{T}_k$ will be divided into categories $\mathscr{T}_k = \{\mathscr{T}_{c_i}^k\}_{i=1}^N$, in which $\mathscr{T}_c^k$ contains N_c^k number of samples. The GPCs competence $\Psi(c,k)$ is estimated as the mean value of the Shannon entropy:

$$\Psi(c,k) = \frac{1}{N_c^k} \sum_{\boldsymbol{t}_c^k \in \mathscr{T}_c^k} \mathscr{H}(c|\boldsymbol{t}_c^k) \tag{4}$$

The higher the $\Psi(c,k)$ is, the more uncertain the robot is about the object.

*2) **Next Object and Next Physical Property Selection**:* Let us define the object-property pair, $\alpha(c,k)$ as a function of the object c ($\mathscr{C} = \{c_i\}_{i=1}^N$) and physical property $k \in$ {texture, stiffness, thermal conductivity} ($\mathscr{T} = \{\mathscr{T}_{k_j}\}_{j=1}^3$). After selecting $\alpha(c,k)$, the robot moves to the object c and executes the corresponding exploratory action to perceive the physical property k. In order to learn about objects efficiently, the robot can greedily sample the next object and the next property which maximize $\Psi(c,k)$ of GPCs (exploitation). In order to avoid being trapped in the local maxima, we add an exploration rate so that the robot can randomly select $\alpha(c,k)$ by following the uniform distribution (exploration). We denote p_α as a probability, which is uniformly generated with $\mathscr{U}(0,1)$ at each iteration in the AT-LPP. Then the next object c^* and next physical property s^* is determined by:

$$\alpha^*(c,k) = \begin{cases} \underset{c_i\in\mathscr{C}, k_j\in\mathscr{K}}{\arg\max}\, \Psi(c_i,k_j), & \text{if } p_\alpha > \varepsilon_\alpha \\ \\ c = \mathscr{U}\{c_1,c_2,...c_N\},\ k = \mathscr{U}\{k_1,k_2,k_3\}, & \text{o.w.} \end{cases} \tag{5}$$

where ε_α is the parameter to control the exploration-exploitation trade-off.

VI. Active Touch for Object Discrimination (AT-OD)

A. Problem Definition

The task of the robot is to perform a sequence of exploratory actions ($\mathscr{A} = \{a_k\}_{k=1}^K$) to efficiently discriminate among objects which have already been learned. However, in this scenario, the objects can have various positions and orientations in the unknown workspace. First the robot explores the workspace using our proposed active pre-touch approach (Sec. III). Then it exploits the objects' prior knowledge (the observation models and training dataset of objects), efficiently constructed by our proposed active tactile object learning strategy (Sec. V), to iteratively apply exploratory actions on objects. We propose a method to enable the robotic system to determine the most informative action at each step, such that the objects can be distinguished with the fewest actions possible.

To start the discrimination process, the object priors $p(c)$ are set to be uniformly distributed. After applying an exploratory movement on the object, the robot perceives a new observation $\boldsymbol{z}$, and updates the object priors through Bayesian inference with the observation probability $p(\boldsymbol{z}|c)$ calculated by GPCs: $p(c|\boldsymbol{z}) \propto p(\boldsymbol{z}|c)\cdot p(c)$. The next exploratory action is then selected and executed, which in turn generates a new observation. This iterative process proceeds until the maximum a posterior (MAP) of the object has reached the expected probability; or the robot has already applied the target number of exploratory actions. The class of the object is determined by the MAP.

B. Optimal Exploratory Action Selection

Intuitively, when the robot applies an exploratory action on an object and perceives its discriminant tactile property, the robot can easily distinguish the object from the others made of different materials. However, if an exploratory action results in confusing observations between objects, it is less useful. Therefore, the advantage of selecting a particular exploratory action can be inferred by how much confusion the action results in. To do this, we measure the confusion of an exploratory action by calculating the objects' similarity, and use it to guide the next action selection. Similar work has been done by Fishel et al [27]. However, their method suffered from the curse of dimensionality. In contrast, our proposed method is unrestricted by the feature dimensions, and thus can be applied to high dimensional features, such as surface texture property and thermal conductivity.

*1) **Objects' Similarity Measurement**:* In order to measure the similarity of object pairs, we exploit the constructed observation models and the efficiently collected training dataset during the active tactile learning process. We denote the similarity between object c_i and c_j when perceiving tactile property k by s_{ij}^k. The similarity between objects can be estimated by the mean value of observation probability $p(c_j|\boldsymbol{t}_{c_i}^k)$ averaged over training samples:

$$s_{ij}^k = \frac{1}{N_{c_i}^k} \sum_{\boldsymbol{t}_{c_i}^k \in \mathscr{T}_{c_i}^k} p(c_j|\boldsymbol{t}_{c_i}^k) \tag{6}$$

with $N_{c_i}^k$ being the number of training samples from the object c_i and the physical property k. s_{ij}^k ranges between 0 (dissimilar) to 1 (similar).

2) Next Action Selection: To select the next exploratory action which produces most discriminant tactile feedback, the similarity (J_{c_i,a_k}) between an object c_i and the others after the robot applies the exploratory action a_k is computed by:

$$J_{c_i,a_k} = \frac{\sum_{c_j\in\mathscr{C}, c_j\neq c_i} p(c_j|\boldsymbol{z}) s_{ij}^k}{\sum_{c_j\in\mathscr{C}} p(c_j|\boldsymbol{z}) s_{ij}^k} \tag{7}$$

with $\boldsymbol{z}$ being the observation perceived by the robot.

The confusion of the exploratory action a_k is then estimated by the expected similarity among all objects: $E(J_{a_k}) = \sum_{c_i\in\mathscr{C}} p(c_i|\boldsymbol{z}) J_{c_i,a_k}$. Finally, the next best exploratory action a^* which provides the lowest confusion is selected: $a^* = \underset{k\in K}{\text{argmin}}\, E(J_{a_k})^{\gamma_k}$. The discount factor γ_k is used to control the exploration-exploitation trade-off. It is proportional to $1/n_k$,

Fig. 5. Experimental objects. The physical properties are evaluated subjectively by human subjects and are indicated in the panel to the upper right of each object (S: stiffness, T: roughness of surface textures, C: thermal conductivity. ++: very high; +: high; O: middle; -:low; –: very low).

with n_k denoting the times the exploratory action a_k has been applied on the object.

VII. Experimental Results

In order to evaluate in real time the performance of our proposed framework which consists of active pre-touch and active touch, we designed two experimental scenarios. In the first scenario, the robotic system was asked to autonomously and efficiently learn about the experimental objects based on their physical properties (stiffness, surface textures, and thermal conductivity). In the second scenario, the task of the robot was to actively discriminate among objects, taking advantage of the prior knowledge of the objects obtained during the active learning process. In both scenarios, the workspace was unknown, and the robot had no knowledge about the number of objects and their positions in it. It is noteworthy to mention that we arbitrarily changed the light intensity when conducting the experiments, in order to show that our framework works well under different light conditions (please watch the video to this study).

A. *Properties of Test Objects*

To assess our proposed framework, we deliberately selected nine objects with different materials (glass, metal, cardboard, and plastic) with regular and irregular textures, and various shapes (triangular, rectangular, cross, and heart shape) (Fig. 5). The physical properties of the objects varied from relatively similar to quite different.

B. *Active Learning about Objects' Physical Properties*

In the first scenario, the robotic system used our proposed active pre-touch method to efficiently explore the unknown workspace. Then, it actively learned about objects by means of their physical properties.

*1) **Active Pre-touch for Workspace Exploration**:* Fig. 6(a) illustrates the workspace, which is a cuboid of $110cm \times 64cm \times 10cm$ $(L \times W \times H)$. A corresponding Cartesian coordinate frame (world coordinate frame) was defined along its length edge (X-axis), width edge (Y-axis), and height edge (Z-axis). This workspace was discretized into $27 \times 24 \times 10$ grid cells. The likelihood of the proximity sensors $p(z_i^n|l^n,d^n)$ was modelled as a Gaussian distribution $\mathcal{N}(\mu,\sigma)$ at each discretized distance $d = [5,4,3,2,1.5,1,0.8,0.5,0.2,0]cm$, in which $\mu = [0.008,0.015,0.028,0.065,0.11,0.25,0.38,0.76,0.93,0.98]$ and $\sigma = [0.03,0.04,0.06,0.1,0.28,0.7,1.2,1.6,0.18,0.09]\cdot 10^{-1}$.

During the exploration, the sensor array (the end-effector of the robot) was held at the maximum height of the workspace and horizontal to the X-Y plane. The performance of our proposed active pre-touch method was compared with the random and uniform strategies which served as baselines. Using the random pre-touch exploration strategy, at each exploration step, the robot randomly selects the next location by following the uniform distribution. We calculated the grid entropy to measure the uncertainty of the workspace during the exploration. To perform the statistical study, each strategy was repeated 10 times. In each experiment the maximum number of robot movements was set to 600. Fig. 6(e) illustrates that using the proposed active pre-touch strategy, the robot reduced its uncertainty about the workspace significantly compared to random and uniform approaches. This is due to the fact that with our proposed method, the robot explored the locations with the higher probability of observing an object. Fig. 6(d)-6(b) illustrates the results of workspace exploration after 300 steps. Fig. 6(b) shows that using our active pre-touch strategy, all of the nine objects were successfully clustered and localized, whereas random and uniform strategies suffered from insufficient exploration of the workspace, yielding either wrong determination of the objects' number or wrong geometry estimation (Fig. 6(d) and 6(c)).

*2) **Active Touch for Learning Physical Properties**:*

***Test Data Collection**:* We evaluated our proposed active learning algorithm with a test database, which was constructed automatically by the robot by performing the three exploratory movements 20 times on each object (pressing, sliding, and static contact). The robot started each exploratory action with light contact with the objects, with the minimum stable contact force that can be measured by the artificial skin ($F_{av} = 0.05N$). The pressing movement consisted of pressing the end-effector with skin cells $2mm$ on the surface of the objects and measuring the total normal force for $3s$. For sliding, the robot slid its artificial skin on the surface of the objects with the constant velocity of $1cm/s$ for $3cm$. To measure the thermal conductivity of objects, the robot made a static contact with the objects, including a light contact and pressing its sensitive part $1mm$ on the the surface for $15s$. Then robot raised its end-effector for $30s$ in order to restore the sensors to ambient temperature. In this way the artificial skin had a similar initial temperature condition in all trials.

***Active Learning about Objects via Three Physical Properties**:* To initialize the active learning process, the robot collected small training samples by performing each of three exploratory actions once on each object. Each step when the robot sampled a new training instance, the recognition accuracy of GPCs was measured with the test dataset. The performance of AT-LPP was compared with the random and uniform strategy. In this regard, the entire experiment was repeated 30 times using each approach. Fig. 7(d) shows that AT-LPP consistently outperforms the other methods by obtaining

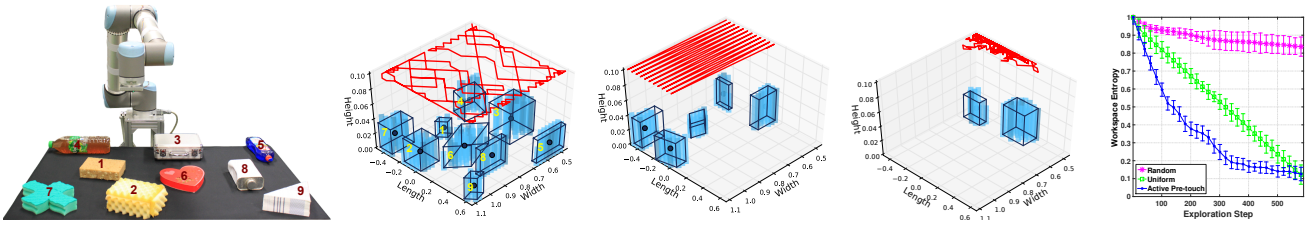

(a) The unknown workspace (b) Active pre-touch (c) Uniform (d) Random (e) Comparison

Fig. 6. **(a)**: The unknown workspace which the robot explored. **(b)-(d)**: Trajectories of the robot's end-effector during the exploration of the workspace and the localization results using three methods. (**b**): Active pre-touch strategy. (**c**): Uniform strategy. (**d**): Random strategy. (**e**): Statistical evaluation of the active pre-touch method with random and uniform strategies. The horizontal axis shows the number of movements the robot has when exploring the workspace. The vertical axis shows the Shannon entropy in the workspace.

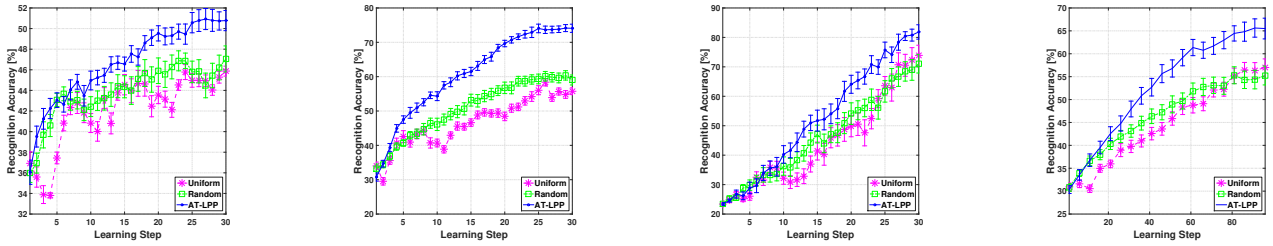

(a) Stiffness (b) Surface textures (c) Thermal conductivity (d) Three physical properties

Fig. 7. **(a)-(c)**: Evaluation of AT-LPP by learning about the experimental objects via one physical property (**a**): Stiffness. (**b**): Surface textures. (**c**): Thermal conductivity. The horizontal axis represents the learning steps (at each step a new training sample is collected), and the vertical axis represents the value of recognition accuracy on the test dataset averaged over 30 runs. (**d**): Evaluation of AT-LPP with three physical properties (stiffness, surface textures, and thermal conductivity).

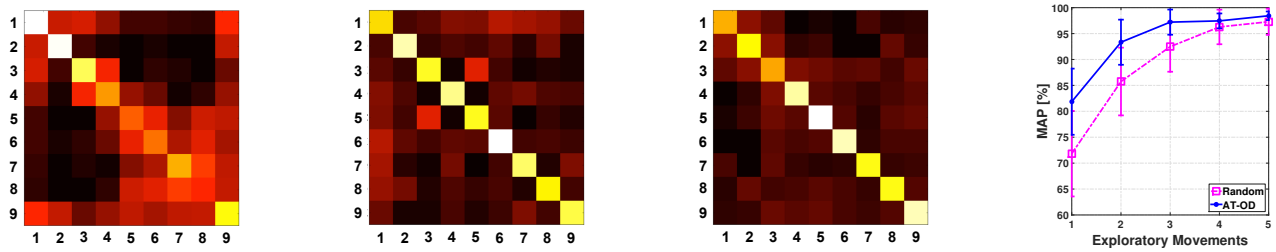

(a) Stiffness (b) Surface texture (c) Thermal conductivity (d) Comparison

Fig. 8. **(a)-(c)**: Visualization of the object similarity by three matrices. The element in each matrix illustrates the value of similarity between object pairs. Light color indicates higher similarity, while dark color refers to lower similarity. (**a**): Similarity matrix for stiffness. (**b**): Similarity matrix for surface textures. (**c**): Similarity matrix for thermal conductivity. (**d**): Evolution of the object MAP during object discrimination process. The active object discrimination method was compared with random method. The horizontal axis shows the number of exploratory movements applied on the objects, and the vertical axis shows the object MAP.

the same recognition accuracy with fewer training samples. For instance, the robot had in average 50% fewer training samples compared to the other methods, when the recognition accuracy reached 55% (Fig. 7(d)). Therefore, the robot following AT-LPP method can construct reliable observation models of objects with efficient training samples.

Active Learning about Objects via One Physical Property: In order to assess further the performance of the AT-LPP algorithm, the robot was additionally asked to learn about objects via one of the three tactile properties individually. Fig. 7(a), 7(b), and 7(c) indicate that the learning progress was dependent on the distributions of the extracted features of the physical properties. Fig. 7(a) shows that learning about objects via their stiffness is more difficult, whereas the learning process for object surface texture and thermal conductivity were faster and resulted in higher recognition accuracy (Fig 7(b) and 7(c)). In all three cases, AT-LPP performs better than random and uniform methods. It can be concluded that using our proposed method (AT-LPP), the robot can efficiently learn about objects even with one modality of its artificial skin.

C. Active Object Discrimination

In this experiment, we evaluated our proposed active touch strategy for object discrimination based on the objects' prior knowledge constructed efficiently in the previous scenario. Before discriminating among objects, the robot actively explored the unknown workspace to localize objects as well as estimate their geometric information, by following the same procedure as described in Section VII-B1. Fig. 8(a), 8(b), and 8(c) illustrates the probabilistic similarity matrices of nine objects for the three tactile properties respectively. The results show that the measured object similarity was

well correlated with the evaluation from human subjects (see Fig. 5). For example, sponge, soft sponge, and toy block were easily distinguished from other objects via their significantly different stiffness (Fig. 8(a)). Conversely, toolbox and tableware detergent were easily confused via their textural properties (Fig. 8(b)), because both of their surface textures are smooth. In general, when discriminating among the experimental objects, the pressing action was less informative as the objects shared similar stiffness (Fig. 8(a)). In contrast, the objects were quite dissimilar based on their textural property and thermal conductivity. Therefore, by applying sliding and static contact, the objects could be more easily recognized. We conducted the experiment to evaluate the performance of our proposed active object discrimination strategy compared with random action selection method. Each approach was repeated 30 trials. In each trial, the robot distinguished each of the nine experimental objects by performing sequentially five exploratory actions on each object. The initial object priors $p(c)$ were first set to be uniformly distributed. After applying each exploratory action, the posterior of an object $p(c|\boldsymbol{z})$ was updated and the object class, which was determined by the MAP, was compared to the true object class. Fig. 8(d) shows the evolution of MAP with growing number of exploratory movements applied on objects. The recognition performance of the proposed AT-OD method is higher than 94% in average with only two exploratory movements. The robotic system using the AT-OD consistently identified objects with higher confidence than selecting random exploratory movements.

VIII. Conclusion

In this study, we proposed a probabilistic tactile-based framework consisting of active pre-touch and active touch methods for robotic systems with multi-modal artificial skin. Using our proposed framework, the robot performed a complete series of tasks, i.e. the exploration of unknown workspaces based on active pre-touch approach, active touch based learning of object's physical properties, and the active object discrimination task. The effectiveness of our proposed framework was evaluated through online experiments and statistical analysis. Results shows that the framework outperforms baseline uniform and random strategies in all the tasks. The active pre-touch strategy presents a maximum entropy reduction of 30% and 70% compare to uniform and random respectively, as well as achieving better estimation of the objects poses. The active touch learning provides high recognition accuracy with fewer samples, reaching 50% of less samples than the baseline strategies. Finally, results show that, by taking advantage of the learned prior knowledge, the autonomous robot efficiently discriminated objects with 10% improvement of recognition accuracy compare to the random action selection approach.

Due to the low spacial resolution provided by the proximity sensors on the artificial skin array, objects which are close to each other in the workspace can hardly be clustered after the exploration. In order to tackle this problem, the spacial resolution of the sensor array can be increased by fusing the proximity information and force signals while contacting the objects.

References

[1] G. Robles-De-La-Torre, "Theimportance of the sense of touch in virtual and real environments," *IEEE Multimedia*, vol. 13, pp. 24–30, 2006.

[2] R. S. Dahiya, G. Metta, M. Valle, and G. Sandini, "Tactile sensing—from humans to humanoids," *IEEE Trans. on Robotic*, vol. 26, no. 1, pp. 1–20, 2010.

[3] P. Dallaire, P. Giguere, and et.al, "Autonomous tactile perception: A combined improved sensing and bayesian nonparametric approach," *Robotics and Autonomous Sys.*, vol. 6, pp. 422–435, 2014.

[4] D. S. Chathuranga, Z. Wang, and e. a. Ho, "A biomimetic soft fingertip applicable to haptic feedback systems for texture identification," *IEEE Int. Symp.on Hapt. Aud. Vis. Env. and Games*, pp. 29–33, 2013.

[5] M. Kaboli, K. Yao, and G. Cheng, "Tactile-based manipulation of deformable objects with dynamic center of mass," *IEEE Int. Conf. on Hum. Robots*, pp. 752–757, 2016.

[6] V. Chu, I. McMahon, and e. a. Riano, "Using robotic exploratory procedures to learn the meaning of haptic adjectives," *IEEE Int. Conf. on Robotics and Automation*, pp. 3048–3055, 2013.

[7] A. Song, Y. Han, H. Hu, and J. Li, "A novel texture sensor for fabric texture measurement and classification," *IEEE Trans. on Instrumentation and Measurement*, vol. 63, no. 7, pp. 1739–1747, 2014.

[8] H. Hu, Y. Han, A. Song, S. Chen, C. Wang, and Z. Wang, "A finger-shaped tactile sensor for fabric surfaces evaluation by 2-dimensional active sliding touch," *Sensors*, vol. Vol. 14, pp. 4899–4913, 2014.

[9] W. Mayol-Cuevas, J. Juarez-Guerrero, and et al., "A first approach to tactile texture recognition," *IEEE Int. Conf. on Systems, Man, and Cybernetics*, vol. 5, pp. 4246–4250, 1998.

[10] K. E. Friedl, A. R. Voelker, A. Peer, and C. Eliasmith, "Human-inspired neurorobotic system for classifying surface textures by touch," *IEEE Robotics and Automation Letters*, vol. 1, pp. 516–523, 2016.

[11] N. F. Lepora, M. Evans, and et al., "Naive bayes texture classification applied to whisker data from a moving robot," *The Int. Joint Conf. on Neural Networks*, pp. 1–8, 2010.

[12] M. Kaboli, R. Walker, and G. Cheng, "Re-using prior tactile experience by robotic hands to discriminate in-hand objects via texture properties," *IEEE Int. Conf. on Robotics and Automation*, pp. 2242–2247, 2016.

[13] M. Kaboli, P. Mittendorfer, V. Hugel, and G. Cheng, "Humanoids learn object properties from robust tactile feature descriptors via multi-modal artificial skin," *IEEE Int. Conf. on Hum. Robots*, pp. 187–192, 2014.

[14] N. H. H. Mohamad Hanif and et al., "Surface texture detection with artificial fingers," *Int. Conf. of Engineering in Medicine and Biology Society*, pp. 8018–8021, 2015.

[15] D. Xu, G. E. Loeb, and J. A. Fishel, "Tactile identification of objects using bayesian exploration," *IEEE International Conference on Robotics and Automation*, pp. 3056–3061, 2013.

[16] N. F. Lepora, U. Martinez-Hernandez, and T. J. Prescott, "Active touch for robust perception under position uncertainty," *IEEE Int.l Conf. on Robotics and Automation*, pp. 3020–3025, 2013.

[17] H. P. Saal, J.-A. Ting, and S. Vijayakumar, "Active sequential learning with tactile feedback." *AISTATS*, pp. 677–684, 2010.

[18] J. A. Fishel and G. E. Loeb, "Bayesian exploration for intelligent identification of textures," *Frontiers in Neuroscience*, 2012.

[19] D. Tanaka, T. Matsubara, K. Ichien, and K. Sugimoto, "Object manifold learning with action features for active tactile object recognition," *IEEE Int. Conf. on Intelligent Robots and Systems*, pp. 608–614, 2014.

[20] U. Martinez-Hernandez, T. J. Dodd, M. H. Evans, T. J. Prescott, and N. F. Lepora, "Active sensorimotor control for tactile exploration," *Robotics and Autonomous Systems*, vol. 87, pp. 15–27, 2017.

[21] P. Mittendorfer and G. Cheng, "Humanoid multimodal tactile-sensing modules," *IEEE Trans. on Robotics*, vol. 27, pp. 401–410, 2011.

[22] P. Lanillos and e. a. Besada-Portas, "Minimum time search in uncertain dynamic domains with complex sensorial platforms," *Sensors*, vol. 14, no. 8, pp. 14 131–14 179, 2014.

[23] P. Lanillos, S. K. Gan, E. Besada-Portas, G. Pajares, and S. Sukkarieh, "Multi-uav target search using decentralized gradient-based negotiation with expected observation," *Inf. Sciences*, vol. 282, pp. 92–110, 2014.

[24] M. Kaboli, R. Walker, and G. Cheng, "In-hand object recognition via texture properties with robotic hands, artificial skin, and novel tactile descriptors," *IEEE Int. Conf. on Hum. Robots*, pp. 2242–2247, 2015.

[25] M. Kaboli and G. Cheng, "Robust tactile descriptors for discriminating objects from textural properties via artificial robotic skin," *IEEE Tans. on Robotics*, p. Submitted, 2017.

[26] C. E. Rasmussen and C. K. I. Williams, "Gaussian processes for machine learning," *The MIT Press*, 2005.

[27] J. Fishel and G. Loeb, "Bayesian exploration for intelligent identification of textures." *Frontiers in neurorobotics*, vol. 6, 2011.